Catalysis Today 249 (2015) 145–152

Contents lists available at ScienceDirect

Catalysis Today

journal homepage: www.elsevier.com/locate/cattod

Effect of the nature of carbon support on the formation of active sites in Pd/C and Ru/C catalysts for hydrogenation of furfural

Roman M. Mironenko[a,b,*], Olga B. Belskaya[a,c], Tatyana I. Gulyaeva[a], Alexander I. Nizovskii[c,d], Alexander V. Kalinkin[d], Valerii I. Bukhtiyarov[d], Alexander V. Lavrenov[a], Vladimir A. Likholobov[a,e]

[a] Institute of Hydrocarbons Processing, Siberian Branch of the Russian Academy of Sciences, Neftezavodskaya Street, 54, 644040 Omsk, Russia
[b] Omsk F.M. Dostoevsky State University, Pr. Mira, 55a, 644077 Omsk, Russia
[c] Omsk State Technical University, Pr. Mira, 11, 644050 Omsk, Russia
[d] Boreskov Institute of Catalysis, Siberian Branch of the Russian Academy of Sciences, Pr. Lavrentieva, 5, 630090 Novosibirsk, Russia
[e] Omsk Scientific Center, Siberian Branch of the Russian Academy of Sciences, Pr. Marksa, 15, 644024 Omsk, Russia

ARTICLE INFO

Article history:
Received 29 July 2014
Received in revised form 14 October 2014
Accepted 16 October 2014
Available online 15 November 2014

Keywords:
Furfural
Catalytic hydrogenation
Palladium catalysts
Ruthenium catalysts
Carbon supports

ABSTRACT

The study considered the formation and catalytic properties of the active sites in Pd/C and Ru/C catalysts supported on carbon nanotubes (CNT) and carbon black (CB). The nature of carbon support was shown to affect the dispersion of supported metal and its catalytic properties in the aqueous-phase hydrogenation of furfural. The 1.5% Pd/CB catalyst demonstrated a high selectivity (99%) for furfuryl alcohol during hydrogenation of furfural at a temperature of 50 °C and hydrogen pressure of 0.5 MPa. The 1.5% Pd/CNT catalyst was not active under mild conditions of the reaction (50 °C, 0.5 MPa), but had a greater tendency to reduce the furan ring under severe conditions (90 °C, 0.5 or 2.0 MPa) as demonstrated by an increased yield of tetrahydrofurfuryl alcohol. The ruthenium samples showed a low activity in aqueous-phase hydrogenation of furfural irrespective of the support nature and reaction conditions, possibly due to irreversible adsorption of water on the active sites.

1. Introduction

Furfuryl alcohol is widely used in chemical industry, mainly for the production of special resins, polymers and coatings on their basis, which are resistant to acids, alkalies and various solvents. In addition, furfuryl alcohol is employed as a diluent for epoxy resins and as a solvent for phenol formaldehyde resins and poorly soluble pigments. In the organic synthesis, furfuryl alcohol is a feedstock for the production of tetrahydrofurfuryl alcohol and 2,3-dihydropyran and an intermediate for the synthesis of lysine, vitamin C, various lubricants and plasticizers [1–4].

In industry, furfuryl alcohol is obtained by catalytic hydrogenation of furfural in a liquid or vapor phase [1,2,5–7]. The liquid-phase process is carried out with copper chromite systems as the catalysts. The main disadvantage of copper chromite catalysts is their toxicity caused by the presence of chromium oxides, which allows considering such catalysts as environmental pollutants [1–4]. Thus, the development of catalysts that are highly active in hydrogenation of furfural to furfuryl alcohol and contain no chromium is a topical task.

By now, various chromium-free compositions have been proposed for selective hydrogenation of furfural [1,3,4]; among them are supported catalysts containing noble metals such as platinum [5,8–10], palladium [5,8,9,11] and ruthenium [8,9,12]. The nature of metallic component and its state in the catalyst are of key importance for hydrogenation processes. It should be noted that hydrogenation of furfural is a structure-sensitive reaction [13–16]: catalyst activity in the formation of furfuryl alcohol improves with increasing the particle size of supported metal.

To provide the desired activity and selectivity of hydrogenation catalyst, the choice of support is also very important because features of the support affect the state of supported metal, the adsorption of reagents, and mass transfer processes [2,17–22]. The use of carbon materials as supports in the synthesis of catalyst for the liquid-phase hydrogenation has some advantages. Carbon supports possess a high specific surface area, a developed pore space, and controllable chemical properties of the surface [22–25].

* Corresponding author at: Institute of Hydrocarbons Processing, Siberian Branch of the Russian Academy of Sciences, Neftezavodskaya Street, 54, 644040 Omsk, Russia. Tel.: +7 3812 670 474; fax: +7 3812 646 156.
E-mail address: ch-mrm@mail.ru (R.M. Mironenko).

http://dx.doi.org/10.1016/j.cattod.2014.10.037
0920-5861/

In the case of hydrogenation in a solution, the composition of products may depend on the nature of solvent. Furfural is produced by the hydrolysis of plant biomass; so, attention was recently drawn to subsequent hydrogenation of furfural in an aqueous solution yielding valuable chemical products [9,12,26–31]. The use of water as a solvent makes it possible to obtain a wide range of products: depending on the chosen conditions and catalyst, water can be an active participant of the reaction.

The goal of this work was to elucidate the effect exerted by the nature of carbon support on the formation of metallic sites in Pd/C and Ru/C catalysts for the aqueous-phase selective hydrogenation of furfural to furfuryl alcohol.

2. Experimental

2.1. Catalyst preparation

Carbon supports used in this study were multi-wall carbon nanotubes (CNT) Baytubes C 150 HP (Bayer) and conductive carbon black (CB) P278-E (analog to N472). Prior to experiments, carbon supports were dried overnight in air at 120 °C to remove the adsorbed water.

During the catalyst synthesis, aqueous solutions of palladium(II) and ruthenium(IV) chloride complexes with a specified concentration were used as the precursors. They were prepared by dissolution of palladium(II) chloride and ruthenium(IV) hydroxytrichloride (both pure grade, Aurat) in concentrated hydrochloric acid (Pd to HCl and Ru to HCl molar ratios of 1:2 and 1:3, respectively) and dilution with water to a desired concentration. The adsorption isotherms of palladium and ruthenium chloride complexes on the chosen supports were obtained by the separate sample method with the support to solution weight ratio of 1:25. The range of metal concentrations in the solutions was equal to 0.2–7.6 g L^{-1}. The adsorption experiments were carried out at ambient temperature. Palladium content in the solutions was estimated by AAS (Shimadzu AA-6300), and ruthenium content – by ICP OES (Varian 710-ES).

The supported ruthenium catalysts with the 1.5 wt% content of metal were obtained by incipient wetness impregnation of the carbon supports with aqueous solutions of ruthenium(IV) chloride complexes. The palladium catalysts with 1.5 wt% Pd were prepared by the adsorption of palladium(II) chloride complexes from excess solution. After the impregnation, both the palladium and ruthenium samples were dried in air at room temperature.

In order to estimate the metal content by AAS (palladium) and ICP OES (ruthenium), the samples were calcined in a muffle furnace at 550 °C and the residues were dissolved.

2.2. Methods of catalyst characterization

Scanning electron microscopic (SEM) images of the carbon supports were taken by a JSM-6460 LV (JEOL) instrument, using Au-coated samples and acceleration voltage of 20 kV.

The texture characteristics of the supports (BET specific surface area, pore adsorption volume, average pore diameter) were obtained on a Sorptomatic-1900 (Fisons Instruments) static volumetric apparatus, using the nitrogen adsorption–desorption at 77.4 K.

Surface acid–base properties of the carbon supports at the solid–liquid interface were estimated by determining the point of zero charge (PZC) according to a method developed by Park and Regalbuto [32]. The samples were placed in aqueous solutions with different initial values of pH. The pH values were measured until the equilibrium was established. Therewith, PZC corresponded to a plateau on the curve of final (equilibrium) pH versus the initial pH. Solutions with the initial pH value ranging from 1 to 13 were prepared with HCl and NaOH. All the measurements were performed using an InLab Easy BNC combined electrode (Mettler Toledo) on a SevenMulti device (Mettler Toledo).

The composition of surface functional groups of CNT and CB was studied using Fourier transform infrared (FTIR) spectroscopy on a Nicolet-5700 (Thermo Fisher Scientific) instrument. Thin carbon films prepared by deposition of CNT or CB on BaF_2 glasses were used as the samples for FTIR spectroscopy [33]. FTIR spectra were recorded in a transmission mode over the range of 850–2000 cm^{-1} with a resolution of 4 cm^{-1}. The assignment of absorption bands was made taking into account the data published in [33–36].

After deposition of the precursor on the supports and drying in air at room temperature, the metal-containing samples were examined in the temperature-programmed reduction (TPR) using an AutoChem II 2920 (Micromeritics) chemisorption analyzer equipped with a thermal conductivity detector (TCD). The TPR experiments were performed with a mixture of 10% H_2 and argon (the flow rate of 25 mL min^{-1}) in a temperature range of 35–400 °C at a heating rate of 10 °C min^{-1}.

Metal dispersion in the Pd/C and Ru/C samples was estimated by pulse chemisorption of CO or O_2 (ruthenium samples) after the catalyst reduction and cooling in an inert gas to the temperature of experiment (room temperature). The 10% CO—He or 10% O_2—He mixture was fed into the flow of inert carrier gas (helium) by pulses at equal time intervals. The batching lasted until the detector signal became constant. The palladium and ruthenium dispersions were calculated taking into account the average adsorption stoichiometry: CO/Pd = 0.5, CO/Ru = 1, O/Ru = 1 [37–39].

Transmission electron microscopic (TEM) images of the Pd/C samples pre-reduced at 250 °C were taken by a JEM-2100 (JEOL) instrument. The samples were prepared by dispersing the catalysts in ethanol and spraying the suspension on a perforated carbon-coated copper grid. TEM images were analyzed using DigitalMicrograph (Gatan) software. The average particle size obtained by statistical treatment of the TEM measurements was recalculated to dispersion value assuming spherical shape as described in [40]:

$$D = 6\frac{V_M/S_M}{d_{av}} \quad (1)$$

where D is the dispersion, V_M is the volume occupied by an atom in bulk metal (0.0147 nm^3 for Pd), S_M is the area occupied by a surface atom (0.0793 nm^2 for Pd) and d_{av} is the average particle size (nm).

X-ray photoelectron spectroscopy (XPS) measurements of the Pd/C samples were carried out in a SPECS photoelectron spectrometer at a residual pressure of 5×10^{-9} Torr in the analyzer chamber. The powdery samples pre-reduced at 250 °C were fixed on a sample holder using a double-side conductive adhesive tape. The samples were introduced in the spectrometer via fast entry lock system. For each sample, spectra were recorded using monochromatic AlK_α radiation ($h\nu$ = 1486.7 eV). Before the measurements, the binding energy (BE) scale of the spectrometer was calibrated against the signal positions of metallic gold and copper, Au $4f_{7/2}$ (84.0 eV) and Cu $2p_{3/2}$ (932.6 eV). The spectra were calibrated with respect to C 1*s* line of the carbon support (284.6 eV) and decomposed into individual components using the XPSPEAK fitting software.

2.3. Catalytic measurements

Pre-treatment of the catalyst samples prior to catalytic experiments included drying in argon at 150 °C for 0.5 h and reduction in a hydrogen flow at 250 °C for 2 h.

Liquid-phase hydrogenation of furfural (99%, Sigma–Aldrich) in the presence of synthesized catalysts was examined using a 180 cm^3 steel autoclave. A 0.5 g catalyst sample was placed in the autoclave with 40 mL of distilled water. To remove air, an argon

flow was passed through the autoclave; after that, the catalyst was pre-reduced with hydrogen at a temperature of 50 °C and pressure of 0.5 MPa for 0.5 h under stirring. After the catalyst pre-reduction, 5.0 mL of furfural and 60 mL of distilled water were loaded into the autoclave. Hydrogenation was performed at a specified temperature and constant hydrogen pressure. The reaction mixture was stirred by a magnetic stirrer at 1400 rpm to prevent external diffusion limitations. The reaction was controlled by measuring the volume of consumed hydrogen with a mass flow meter. The volume of consumed hydrogen normalized to normal conditions was recalculated to its equivalent amount that is needed for the formation of furfuryl alcohol from furfural. After completion of the reaction and cooling, the aqueous phase was separated from the catalyst by filtering.

The products of furfural hydrogenation were identified by ^{1}H NMR, ^{13}C NMR (Bruker Avance-400) and GC–MS (Agilent 5973N/6890N). The quantitative determination of the reaction products was carried out by GC (Hewlett Packard 5890 Series II) in a capillary column HP-PONA (50 m × 0.20 mm, Agilent Technologies) with linear heating from 40 to 200 °C during analysis.

Furfural conversion X (%) and furfuryl alcohol selectivity S (%) were determined as follows:

$$X = \frac{C_{F,0} - C_F}{C_{F,0}} \times 100 \quad (2)$$

$$S = \frac{C_{FA}}{X} \times 100 \quad (3)$$

where $C_{F,0}$, C_F and C_{FA} are the concentrations (wt%) of furfural before the reaction, furfural after the reaction, and furfuryl alcohol, respectively.

3. Results and discussion

3.1. The formation of metallic sites in Pd/C and Ru/C catalysts

As follows from the SEM study (Fig. S1 in the Supplementary materials), chosen carbon materials have different morphology: in distinction to CNT, the CB support consists of the aggregated globular particles. It is well known that the pore structure and acid–base properties of the support play important role in the process of formation of the active surface of the catalyst. From analysis of data given in Table S1 (Supplementary materials), it follows that the difference between CNT and CB involves the lower specific surface area of the CNT sample along with a large average pore size. Evaluation of the acid–base properties of the carbon supports (Fig. S2 in the Supplementary materials) showed that the surface of CB is more acidic (PZC = 6.1) than the surface of CNT (PZC = 7.7). According to FTIR spectroscopy (Fig. S3 in the Supplementary materials), the surface of CNT is extremely poor in the functional groups as compared to CB, the surface of which is characterized by the presence of phenol (C—O stretch at 1000–1220 cm^{-1}), ether (C—O—C stretch at 1150–1250 cm^{-1}), lactone (C—O stretch at 1160–1370 cm^{-1} and at 1675–1790 cm^{-1}), quinone (C=O stretch at 1550–1680 cm^{-1}), carboxyl (C—O stretch at 1120–1200 cm^{-1} and C=O stretch at 1665–1760 cm^{-1}) and anhydride (C—O stretch at 980–1300 cm^{-1} and C=O stretch at 1740–1880 cm^{-1}) groups. Carboxyl, anhydride, quinone and lactone groups are acidic [23] and their presence explains the relatively low PZC value of CB. These groups decrease the hydrophobicity of the carbon, making the surface more accessible for the aqueous solution of the metal precursor. Phenols and ethers are weakly acidic or neutral. It has been found that these oxygen groups increase the interaction of the metal precursor with the support [23].

Adsorption properties of the supports with respect to palladium(II) chloride complexes were studied and isotherms of $H_2[PdCl_4]$ adsorption from aqueous solutions were obtained

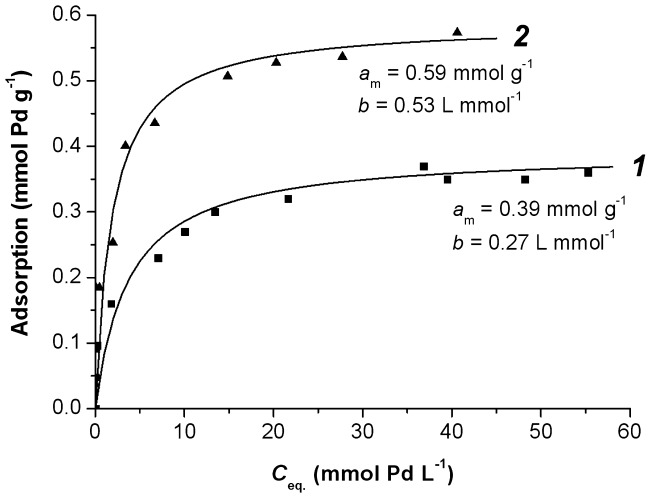

Fig. 1. Isotherms of $H_2[PdCl_4]$ adsorption on CNT (1) and CB (2).

(Fig. 1). According to the analysis of results by linear anamorphosis method, the adsorption isotherms are described satisfactorily by the Langmuir equation.

A comparison of the equation parameters estimated from the analysis of isotherms (adsorption capacity a_m and adsorption equilibrium constant b) showed that the CB support has higher values of a_m and b (Fig. 1). A maximum amount of palladium in the complexes bound to this support was 6.3 wt%. The CNT support possessed a lower adsorption capacity and a maximum amount of adsorbed palladium was equal to 4.1 wt%.

TPR is the valuable tool for estimating not only the optimal reduction temperature, but also the strength of the metal complex–support interaction. The TPR profiles of the palladium samples have a single hydrogen consumption region up to about 200 °C (Fig. 2), which is attributed to the reduction of the chloride precursor adsorbed on the support surface. According to the chemisorption data (Fig. 1), the CNT support is characterized by a less strong adsorption of $H_2[PdCl_4]$ as compared to CB, that is most likely due to a very low concentration of oxygen groups on the surface of CNT (see Fig. S3 in the Supplementary materials). As a result, the supported complexes are reduced at a lower temperature (the temperature maximum on the TPR profile corresponds to 113 °C). In this case, dispersion of the emerging palladium particles is 36 % (Table 1). A stronger adsorption of $H_2[PdCl_4]$ on the CB surface as compared to CNT leads to a more severe reduction conditions of the precursor (the temperature maximum on the

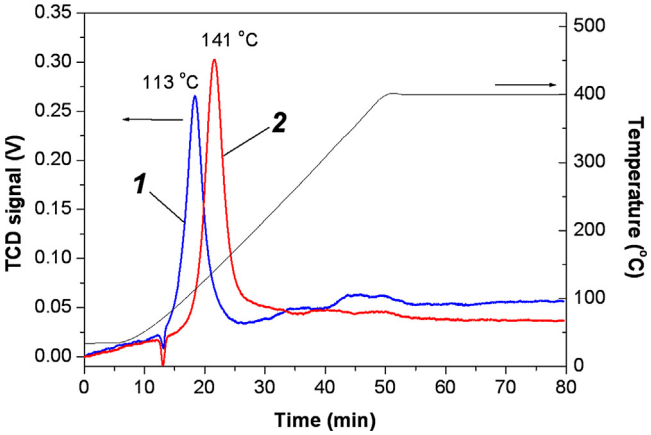

Fig. 2. TPR profiles of palladium chloride complexes adsorbed on the carbon supports: 1.5% Pd/CNT (1) and 1.5% Pd/CB (2).

Table 1
Dispersion of palladium and ruthenium in Pd/C and Ru/C samples, as determined by pulse chemisorption of CO and O_2 at room temperature, and catalytic properties of the samples in aqua-phase hydrogenation of furfural under hydrogen pressure. Prior to catalytic experiments, the catalysts were dried in argon at 150 °C for 0.5 h and reduced in flowing hydrogen at 250 °C for 2 h.

Catalyst	D_{CO} (%)[a]	D_{O_2} (%)[a]	Reaction conditions			H_2 uptake (equiv.)	X (%)	S (%)
			Entry	T (°C)	P (MPa)			
1.5% Pd/CNT	36	–	1	50	0.5	0.01	0	–
			2	90	0.5	0.75	58	87
			3	50	2.0	0.34	40	97
			4	90	2.0	1.85	95	52
1.5% Pd/CB	16	–	5	50	0.5	0.28	29	99
			6	90	0.5	0.57	42	89
			7	50	2.0	0.47	46	98
			8	90	2.0	1.02	76	82
1.5% Ru/CNT	30	42	9	50	0.5	0.02	5	100
			10	90	0.5	0.02	8	100
			11	90	2.0	0.06	14	88
1.5% Ru/CB	62	67	12	50	0.5	0.04	–	–
			13	90	0.5	0.02	–	–
			14	90	2.0	0.09	5	63
			15[b]	50	0.5	0.11	23	63

[a] The dispersion was determined after TPR. The calculation was made for the following adsorption stoichiometry: CO/Pd = 0.5, CO/Ru = 1, O/Ru = 1 [37–39].
[b] Hydrogenation was carried out in ethanol medium.

TPR profile corresponds to 141 °C) and to the formation of particles with a lower dispersion as compared to Pd/CNT (Table 1). A hydrogen evolution peak at 70 °C on the TPR profile (Fig. 2) is caused by decomposition of palladium hydride, which is formed at a low temperature (less than 25 °C) as a result of heterolytic cleavage of the bond in the hydrogen molecule and interaction with the supported palladium complexes [41,42].

As can be seen from TEM image of the 1.5% Pd/CNT sample (Fig. 3a), the palladium particles have mainly a spherical shape and its average size is equal to 2.3 nm, which corresponds to dispersion value of 48%. This value is somewhat higher than that estimated by chemisorption of CO. A discrepancy between TEM and chemisorption data can be explained by the following reasons. First, CO adsorbs on Pd with a variable stoichiometry, which is influenced by the metal dispersion and the nature of the support. The CO/Pd stoichiometry of 1/2 assumed for calculation of metal dispersion might not be representative of the CO adsorption modes, since lower stoichiometries (e.g., 1/3) have also been reported for the CO–Pd systems [43,44]. Second, the high temperature pre-reduction can lead to a partial coverage of Pd particles by the support as has been shown for various Pd/C catalysts [45,46]. This encapsulation could also account for the lower chemisorption uptake than would be expected based on the TEM measurements.

Unfortunately, it was not possible to correctly determine the average particle size of Pd in the 1.5% Pd/CB sample because of very blurred edges of the particles in TEM images (Fig. 3b) and very wide size distribution. Therefore, the properties and behavior of the palladium samples are further explained on the basis of CO chemisorption data.

XPS was used to estimate the oxidation state of supported palladium in the reduced Pd/C samples. The Pd $3d_{3/2}$ and Pd $3d_{5/2}$ core level spectra of each sample can be decomposed into two overlapping peaks (Fig. 4) that indicate the existence of palladium species with different electronic state. The positions of the signals with lower BE values (336.2 and 335.9 eV in the $3d_{5/2}$ region, Table 2) are close to those observed for metallic palladium (BE = 335.7 ± 0.3 eV [47,48]). The signals at 337.9 and 337.2 eV ($3d_{5/2}$) can be assigned to the electron-deficient palladium species $Pd^{\delta+}$ (BE = 337.9 ± 0.3 eV for $PdCl_2$ [47,48]). According to the XPS data, the Pd^0:$Pd^{\delta+}$ atomic ratio is lower for the Pd/CNT sample as compared to Pd/CB. This may be due to the increased content of oxygen in Pd/CNT (Table 2). We speculate that chlorine detected in this sample in very small amount is localized on the support surface only and possibly does not affect (or insignificantly affects) the electronic and dispersion state of supported palladium.

The shift in the BE values of Pd $3d_{5/2}$ core level is probably related to the difference in palladium dispersions, which were estimated by pulse chemisorption. For the more dispersed Pd/CNT sample, the BE values of the Pd^0 and $Pd^{\delta+}$ lines are, respectively, 0.3 and 0.7 eV higher than those for the Pd/CB sample. A similar relation between the values of BE and particle size for both the supported and unsupported metals was described in a number of papers [48–51] and may be attributed to the lattice distortion with decreasing the particle size, which leads to changes in the chemical bonding. It should be noted that a higher dispersion of Pd/CNT as compared to Pd/CB is also indicated by the higher value of Pd:C atomic ratio (Table 2).

The Ru/C catalysts were prepared by incipient wetness impregnation of the carbon supports with aqueous solutions of ruthenium(IV) chloride complexes because a preliminary study revealed that both the CNT and CB possess a very low adsorption capacity with respect to such octahedral complexes (unlike palladium(II) square complexes), a maximum amount of ruthenium on these supports did not exceed 0.28 wt%.

The formation of metallic sites in the Ru/C samples was determined by TPR. At least two hydrogen consumption regions with the maxima at ~110 and ~180 °C (Fig. 5) can be distinguished on the

Table 2
Results of XPS analysis of Pd/C catalysts.

Sample	Pd $3d_{5/2}$ binding energy (eV)		Atomic ratios			
	Pd^0	$Pd^{\delta+}$	Pd^0:$Pd^{\delta+}$	Pd:C	Cl:C	O:C
1.5% Pd/CNT	336.2	337.9	1.0	0.0031	0.0009	0.026
1.5% Pd/CB	335.9	337.2	1.3	0.0016	0	0.013

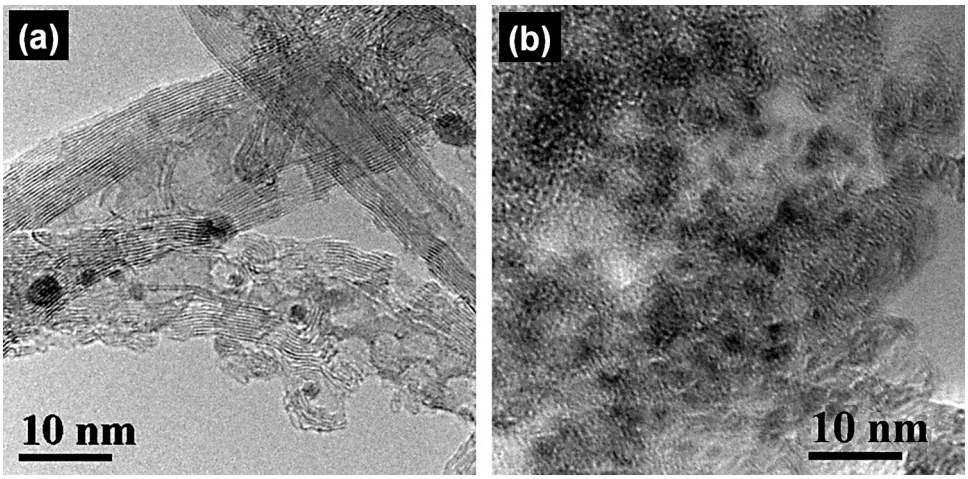

Fig. 3. TEM images of 1.5% Pd/CNT (a) and 1.5% Pd/CB (b) samples.

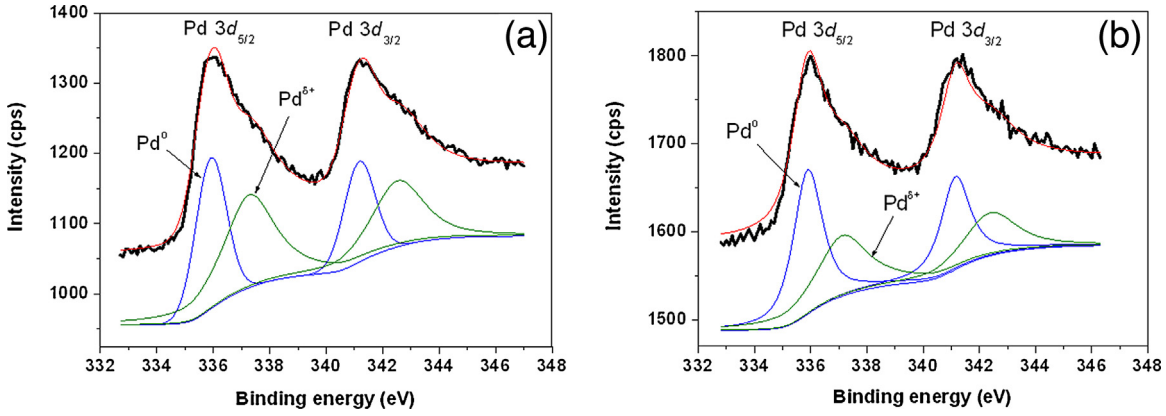

Fig. 4. Pd 3*d* spectra of 1.5% Pd/CNT (a) and 1.5% Pd/CB (b) with decomposition into components. Before measurements, the samples were reduced in flowing hydrogen at 250 °C.

TPR profiles; they may correspond to the reduction of supported species, differing either in the chemical composition (hydrolysis products) or in the strength of interaction with the support [52,53]:

$$[Ru_xO_yCl_z] + \left(y + \frac{z}{2}\right) H_2 \rightarrow xRu^0 + zHCl + yH_2O \quad (4)$$

It should be noted that the fraction of species reduced at the highest temperature is increased in the Ru/CNT sample. Most likely,

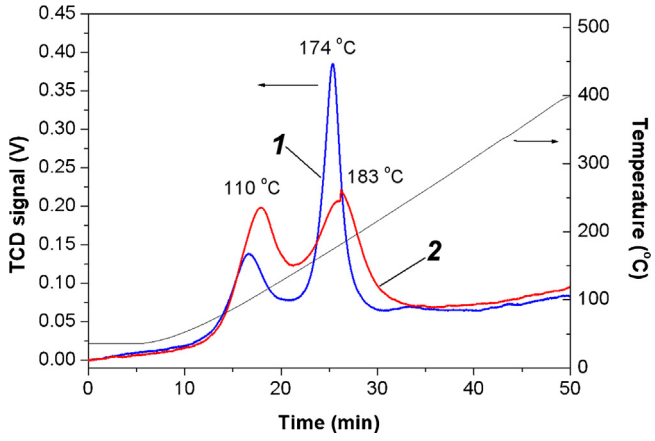

Fig. 5. TPR profiles of ruthenium chloride complexes deposited on the carbon supports: 1.5% Ru/CNT (1) and 1.5% Ru/CB (2).

the observed distinction in the reduction of ruthenium compounds supported on CNT and CB is due to the differences in the composition of surface functional coverage of the supports (see Fig. S3 in the Supplementary materials). So, the composition and therefore reduction of Ru compounds formed after interactions with the surface of different supports may vary.

Dispersion of ruthenium is commonly determined by pulse chemisorption of various probe molecules: CO, H_2, O_2, N_2O [18,38,39,54–57]. However, in the study of carbon-based ruthenium catalysts, the application of some adsorbates produces significant errors in chemisorption measurements (for example, hydrogen adsorption is often accompanied by spillover) [18,39]. In recent years, it was recommended that ruthenium dispersion in Ru/C catalysts should be determined from pulse chemisorption of oxygen at room or lower temperatures [39,56].

In the present work, to avoid possible inaccuracies, ruthenium dispersion in the Ru/C samples was found by pulse chemisorption of CO and O_2 at room temperature. According to the data obtained, the reduction of a precursor in the Ru/CNT sample leads to the formation of ruthenium particles with a lower dispersion as compared to Ru/CB (Table 1). This may be due to an increased fraction of supported complexes reduced at a higher temperature in the Ru/CNT sample (the maximum at 174 °C on the TPR profile, Fig. 5). Dispersion of ruthenium, as measured from CO chemisorption, is somewhat lower than the dispersion estimated from O_2 chemisorption, especially for the Ru/CNT sample. A possible reason is that CO chemisorption on ruthenium produces not only terminal but also

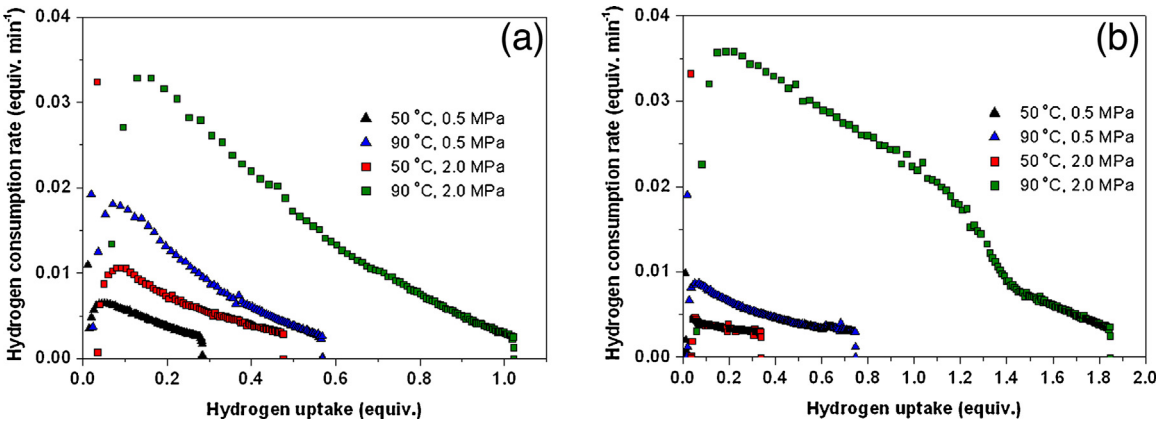

Fig. 6. Hydrogen consumption rate vs. hydrogen uptake during aqueous-phase hydrogenation of furfural over 1.5% Pd/CB (a) and 1.5% Pd/CNT (b) at various temperature and pressure.

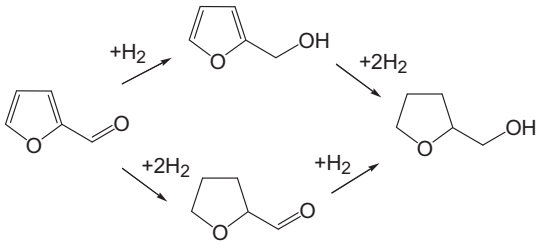

Scheme 1. Possible reaction pathways of furfural hydrogenation.

bridge species [18]. In this case, the CO/Ru ratio changes in a wide range (0.2–1.5).

Thus, more dispersed palladium particles are formed on the surface of CNT, while more dispersed ruthenium particles – on the surface of CB. In any case, the higher the fraction of the species reduced in high-temperature region, the lower the dispersion of the particles formed. Different effect of the support on the dispersions of palladium and ruthenium may be related to distinctions in the preparation conditions: the Pd/C catalysts were synthesized by adsorption of a precursor on the support from excess solution (which was accompanied by chemical binding), while the Ru/C samples – by incipient wetness impregnation. In the latter case, the particle size of supported metal is determined mostly by the texture, and highly dispersed particles are formed on the support with a more developed pore structure, i.e. on CB (see Table S1 in the Supplementary materials).

3.2. The properties of Pd/C and Ru/C catalysts in hydrogenation of furfural

The catalysts containing 1.5% Pd or Ru were examined in the aqueous-phase hydrogenation of furfural at different temperatures (50 and 90 °C) and hydrogen pressures (0.5 and 2.0 MPa). Even under mild conditions (50 °C, 0.5 MPa), hydrogenation of furfural in the presence of the 1.5% Pd/CB catalyst resulted in a highly selective (99%) formation of furfuryl alcohol at a furfural conversion of 29% (Table 1). Raising the pressure (at the temperature of 50 °C) produced more than a 1.5-fold increase in the conversions of hydrogen and furfural (Fig. 6a, Table 1), while selectivity for furfuryl alcohol remained at a high level (98%). Temperature elevation increased the reaction rate and thus the conversions of hydrogen and furfural (Fig. 6a, Table 1). Therewith, as revealed by the analysis of catalyzate, selectivity for furfuryl alcohol decreased due to increasing the role of side reactions related to the hydrogenation of the furan ring. The formation of tetrahydrofurfuryl alcohol (Scheme 1) possibly occurred by further hydrogenation of both furfuryl alcohol and tetrahydrofurfural [8,16,17,27,58].

Although the surface of 1.5% Pd/CNT sample was accessible to the reactants (Table 1), this sample was not active in hydrogenation of furfural under mild conditions of the reaction (50 °C, 0.5 MPa). Only when the temperature or hydrogen pressure was increased, the conversion of furfural over this sample was observed (Table 1, Fig. 6b). Therewith, high selectivity for furfuryl alcohol (97% at a 40% conversion) was attained at a temperature of 50 °C and pressure of 2.0 MPa. Under the most severe conditions used in the work (90 °C, 2.0 MPa), the amount of consumed hydrogen was nearly 2-fold greater than the amount required for the formation of furfuryl alcohol. Along with this, selectivity for furfuryl alcohol decreased substantially, to 52%. Tetrahydrofurfuryl alcohol prevailed among the by-products.

The observed gradual decrease in the reaction rate with increasing conversion (for both the samples, Fig. 6) may be caused by blocking the catalyst active sites by the reaction products. Earlier it was found [5,16,17] that catalyst poisoning during the hydrogenation of furfural (and hence a decrease in the reaction rate) can be attributed to strong adsorption of furfuryl and tetrahydrofurfuryl alcohols on the surface active sites.

Different activity of the Pd/CNT and Pd/CB catalysts in aqueous-phase hydrogenation of furfural can be attributed to the distinctions in the electronic and dispersion states of supported metal. Earlier it was shown that catalyst activity in the hydrogenation of furfural to furfuryl alcohol decreases with decreasing the particle size of supported metal [13–16]. As the size of metal particles increases, the area of the (1 1 1) edges on which adsorption involving the C=O bond is preferred may also increase. Adsorption on fine particles preferentially involves the C=C bond, which improves the selectivity of saturated compounds [59]. Besides, during hydrogenation the activation of hydrogen molecule and cleavage of the H—H bond are more easily done on metal sites with a high amount of available electrons in the external *d* orbital, i.e. electron-rich or totally reduced species, but should be less likely on electron-deficient metal sites [60,61]. Thus, lack of activity of the Pd/CNT sample under mild conditions of the reaction may be due to a higher dispersion of palladium (Table 1) and a lower Pd^0:$Pd^{\delta+}$ atomic ratio (Table 2) as compared to the Pd/CB catalyst. For the same reason, Pd/CNT has a greater tendency to activate the C=C bonds of the furan ring under severe conditions of the reaction as demonstrated by an increased yield of tetrahydrofurfuryl alcohol.

The ruthenium samples showed a low activity in hydrogenation of furfural under the chosen conditions of the reaction. A maximum amount of consumed hydrogen did not exceed 9% of the amount needed for the formation of furfuryl alcohol by stoichiometry, and

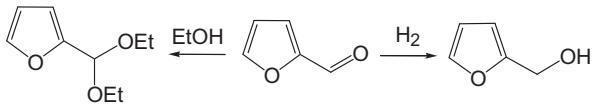

Scheme 2. Reaction pathways of furfural hydrogenation in ethanol medium.

conversion of furfural was not higher than 14% (Table 1). This result is unexpected because ruthenium is commonly considered as an appropriate catalyst for selective reduction of the carbonyl group of ketones and aldehydes [18,19,62]. As shown in our earlier study [63], the 1.5% Ru/CNT and 1.5% Ru/CB samples are active in hydrogenation of benzaldehyde to benzyl alcohol in ethanol medium even at a temperature of 40 °C and pressure of 0.5 MPa. Under the indicated conditions, conversion of benzaldehyde attained 58%.

Different activity of the same Ru/C catalysts in the reactions of benzaldehyde and furfural hydrogenation can be attributed to the effect of solvent. In the present work, water served as a solvent. As shown in [18,64], water can be adsorbed on the ruthenium surface by dissociative mechanism. The H_2O–Ru interaction is much stronger than the H_2O–Pd one [65]. Water that was irreversibly chemisorbed on ruthenium is not displaced from the surface by hydrogen, which is adsorbed, occupying only less active sites.

This assumption was confirmed by a special experiment on hydrogenation of furfural over one of the ruthenium samples in ethanol medium. Even under mild conditions (50 °C, 0.5 MPa), hydrogenation of furfural in the presence of the 1.5% Ru/CB catalyst occurred with a notable conversion (Table 1, entry 15).

The reaction products consisted only of furfuryl alcohol and furfural diethyl acetal (Scheme 2). The latter resulted from the interaction of furfural and ethanol with the involvement of acid sites of the support [66–68].

4. Conclusions

The study has revealed that the nature of carbon support affects the formation and state of supported metal. The adsorption of palladium(II) chloride complexes on CNT is less strong than their adsorption on CB. As a result, Pd complexes supported on CNT are reduced at a lower temperature with the formation of highly dispersed particles and a lower Pd^0:$Pd^{\delta+}$ atomic ratio.

The 1.5% Pd/CB catalyst demonstrated a high selectivity (no less than 98%) for furfuryl alcohol during hydrogenation of furfural at a temperature of 50 °C and hydrogen pressure of 0.5 and 2.0 MPa (the furfural conversion of 29 and 46%, respectively). The 1.5% Pd/CNT sample was inactive under mild reaction conditions (50 °C, 0.5 MPa). However, the conversion of furfural was observed when the temperature or hydrogen pressure was raised, high selectivity for furfuryl alcohol being attained at a temperature of 50 °C and pressure of 2.0 MPa. For both Pd/C samples, raising the temperature increased the conversion of furfural, but selectivity for furfuryl alcohol decreased due to hydrogenation of the furan ring.

The adsorption capacity of CNT and CB with respect to ruthenium(IV) chloride complexes is very low. The incipient wetness impregnation method made it possible to reveal an effect of the support nature on the metal dispersion. The reduction of a precursor in the Ru/CB sample led to the formation of ruthenium particles having a higher dispersion as compared to Ru/CNT.

At the same time, the ruthenium samples showed a low activity in aqueous-phase hydrogenation of furfural irrespective of the support nature and reaction conditions, although the metal surface was accessible to the reactants. This may be due to irreversible adsorption of water on the metallic sites. Application of another solvent (as shown for ethanol) and more severe reaction conditions may improve the catalytic activity of ruthenium-containing samples.

Acknowledgements

The authors are grateful to O.V. Maevskaya for participation in the catalyst preparation, to T.V. Kireeva and A.V. Shilova for determination of palladium and ruthenium content in the impregnating solutions and samples by AAS and ICP OES, to V.P. Talsi, S.N. Evdokimov and E.N. Kudrya for their help with identification of hydrogenation products by NMR and GC–MS, to A.B. Arbuzov for recording FTIR spectra of carbon supports and to M.V. Trenikhin for characterization of palladium catalysts by TEM. We also thank Dr. V.A. Drozdov for useful discussions.

Appendix A. Supplementary data

Supplementary data associated with this article can be found, in the online version, at http://dx.doi.org/10.1016/j.cattod.2014.10.037.

References

[1] H.E. Hoydonckx, W.M. van Rhijn, W. van Rhijn, D.E. de Vos, P.A. Jacobs, Furfural and derivatives, Ullmann's Encyclopedia of Industrial Chemistry, Wiley-VCH, Weinheim, 2012, pp. 285–313.
[2] H.F. Rase, Handbook of Commercial Catalysts. Heterogeneous Catalysts, CRC Press, Boca Raton, 2000.
[3] P. Mäki-Arvela, B. Holmbom, T. Salmi, D.Y. Murzin, Catal. Rev. 49 (2007) 197–340.
[4] B.M. Nagaraja, V. Siva Kumar, V. Shasikala, A.H. Padmasri, B. Sreedhar, B. David Raju, K.S. Rama Rao, Catal. Commun. 4 (2003) 287–293.
[5] M.V. Shimanskaya, Z.G. Yuskovets, V.V. Stonkus, V.A. Slavinskaya, D.R. Kreile, A.A. Avots, Kontaktnye reaktsii furanovykh soedinenii (Contact Reactions of Furan Compounds), Zinatne, Riga, 1985 (in Russian).
[6] M. Shimanskaya, É. Lukevits, Chem. Heterocycl. Compd. 29 (1993) 1000–1011.
[7] K.J. Zeitsch, The Chemistry and Technology of Furfural and its Many By-Products, Elsevier, Amsterdam, 2000.
[8] N. Merat, C. Godawa, A. Gaset, J. Chem. Technol. Biotechnol. 48 (1990) 145–159.
[9] M. Hronec, K. Fulajtarová, T. Liptaj, Appl. Catal. A: Gen. 437–438 (2012) 104–111.
[10] P.D. Vaidya, V.V. Mahajani, Ind. Eng. Chem. Res. 42 (2003) 3881–3885.
[11] S. Sitthisa, T. Pham, T. Prasomsri, T. Sooknoi, R.G. Mallinson, D.E. Resasco, J. Catal. 280 (2011) 17–27.
[12] V.V. Ordomsky, J.C. Schouten, J. van der Schaaf, T.A. Nijhuis, Appl. Catal. A: Gen. 451 (2013) 6–13.
[13] V. Vetere, A.B. Merlo, J.F. Ruggera, M.L. Casella, J. Braz. Chem. Soc. 21 (2010) 914–920.
[14] V.V. Pushkarev, N. Musselwhite, K. An, S. Alayoglu, G.A. Somorjai, Nano Lett. 12 (2012) 5196–5201.
[15] K. An, N. Musselwhite, G. Kennedy, V.V. Pushkarev, R.L. Baker, G.A. Somorjai, J. Colloid Interface Sci. 392 (2013) 122–128.
[16] Y. Nakagawa, K. Takada, M. Tamura, K. Tomishige, ACS Catal. 4 (2014) 2718–2726.
[17] D.V. Sokolsky, Gidrirovanie v rastvorakh (Hydrogenation in Solutions), Nauka, Alma-Ata, 1979 (in Russian).
[18] G.D. Zakumbaeva, N.A. Zakarina, L.A. Beketaeva, V.A. Naidin, Metallicheskie katalizatory (Metal Catalysts), Nauka, Alma-Ata, 1982 (in Russian).
[19] P.L. Rylander, Catalytic Hydrogenation over Platinum Metals, Academic Press, New York, 1967.
[20] P.L. Rylander, Hydrogenation Methods, Academic Press, London, 1985.
[21] S. Nishimura, Handbook of Heterogeneous Catalytic Hydrogenation for Organic Synthesis, John Wiley & Sons, New York, 2001.
[22] A.P.G. Kieboom, F. van Rantwijk, Hydrogenation and Hydrogenolysis in Synthetic Organic Chemistry, Delft University Press, Delft, 1977.
[23] M.L. Toebes, J.A. van Dillen, K.P. de Jong, J. Mol. Catal. A: Chem. 173 (2001) 75–98.
[24] F. Rodríguez-Reinoso, Carbon 36 (1998) 159–175.
[25] F. Rodríguez-Reinoso, A. Sepúlveda-Escribano, in: F. Serp, J.L. Figueiredo (Eds.), Carbon Materials for Catalysis, John Wiley & Sons, Hoboken, 2009, pp. 131–155.
[26] Y. Nakagawa, K. Tomishige, Catal. Commun. 12 (2010) 154–156.
[27] Z. Xinghua, W. Tiejun, M. Longlong, W. Chuangzhi, Fuel 89 (2010) 2697–2702.
[28] M. Hronec, K. Fulajtarová, Catal. Commun. 24 (2012) 100–104.
[29] M. Tamura, K. Tokonami, Y. Nakagawa, K. Tomishige, Chem. Commun. 49 (2013) 7034–7036.
[30] Y. Yang, Z. Du, Y. Huang, F. Lu, F. Wang, J. Gao, J. Xu, Green Chem. 15 (2013) 1932–1940.
[31] S. Liu, Y. Amada, M. Tamura, Y. Nakagawa, K. Tomishige, Green Chem. 16 (2014) 617–626.
[32] J. Park, J.R. Regalbuto, J. Colloid Interface Sci. 175 (1995) 239–252.
[33] L.G. Pyanova, L.S. Luzyanina, V.A. Drozdov, A.V. Veselovskaya, A.B. Arbuzov, V.A. Likholobov, Prot. Met. Phys. Chem. Surf. 46 (2010) 320–324.
[34] P.E. Fanning, M.A. Vannice, Carbon 31 (1993) 721–730.

[35] R.C. Bansal, M. Goyal, Activated Carbon Adsorption, CRC Press, Boca Raton, 2005.
[36] T.J. Bandosz, in: F. Serp, J.L. Figueiredo (Eds.), Carbon Materials for Catalysis, John Wiley & Sons, Hoboken, 2009, pp. 45–92.
[37] G. Fagherazzi, P. Canton, P. Riello, N. Pernicone, F. Pinna, M. Battagliarin, Langmuir 16 (2000) 4539–4546.
[38] A. Maroto-Valiente, M. Cerro-Alarcón, A. Guerrero-Ruiz, I. Rodríguez-Ramos, Appl. Catal. A: Gen. 283 (2005) 23–32.
[39] I. Rossetti, N. Pernicone, L. Forni, Appl. Catal. A: Gen. 248 (2003) 97–103.
[40] G. Bergeret, P. Gallezot, in: G. Ertl, H. Knözinger, F. Schüth, J. Weitkamp (Eds.), Handbook of Heterogeneous Catalysis, Wiley-VCH, Weinheim, 2008, pp. 738–765.
[41] C. Amorim, M.A. Keane, J. Colloid Interface Sci. 322 (2008) 196–208.
[42] O.B. Bel'skaya, T.I. Gulyaeva, A.B. Arbuzov, V.K. Duplyakin, V.A. Likholobov, Kinet. Catal. 51 (2010) 105–112.
[43] E. Gillet, S. Channakhone, V. Matolin, M. Gillet, Surf. Sci. 152–153 (1985) 603–614.
[44] H.N. Pham, Y.J. Pagan-Torres, J.C. Serrano-Ruiz, D. Wang, J.A. Dumesic, A.K. Dutye, Appl. Catal. A: Gen. 397 (2011) 153–162.
[45] N. Krishnankutty, M.A. Vannice, J. Catal. 155 (1995) 312–326.
[46] J.M.M. Tengco, Y.K. Lugo-José, J.R. Monnier, J.R. Regalbuto, Catal. Today (2014), http://dx.doi.org/10.1016/j.cattod.2014.07.006 (in press).
[47] G. Kumar, J.R. Blackburn, R.G. Albridge, W.E. Moddeman, M.M. Jones, Inorg. Chem. 11 (1972) 296–300.
[48] L.V. Nosova, M.V. Stenin, Y.N. Nogin, Y.A. Ryndin, Appl. Surf. Sci. 55 (1992) 43–48.
[49] Y. Takasu, R. Unwin, B. Tesche, A.M. Bradshaw, M. Grunze, Surf. Sci. 77 (1978) 219–232.
[50] B. Richter, H. Kuhlenbeck, H.-J. Freund, P.S. Bagus, Phys. Rev. Lett. 93 (2004) 026805.
[51] S.K. Sengar, B.R. Mehta, Govind, J. Appl. Phys. 115 (2014) 124301.
[52] G.R. Tauszik, G. Leofanti, S. Galvagno, J. Mol. Catal. 25 (1984) 357–366.
[53] S. Galvagno, C. Crisafulli, R. Maggiore, G.R. Tauszik, A. Giannetto, J. Therm. Anal. 30 (1985) 611–618.
[54] K. Lu, B.J. Tatarchuk, J. Catal. 106 (1987) 166–175.
[55] S.K. Masthan, K.V.R. Chary, P.K. Rao, J. Catal. 124 (1990) 289–292.
[56] Z. Kowalczyk, S. Jodzis, W. Raróg, J. Zieliński, J. Pielaszek, A. Presz, Appl. Catal. A: Gen. 184 (1999) 95–102.
[57] J. Okal, Catal. Commun. 11 (2010) 508–512.
[58] L. Baijun, L. Lianhai, W. Bingchun, C. Tianxi, K. Iwatani, Appl. Catal. A: Gen. 171 (1998) 117–122.
[59] A.Y. Stakheev, I.S. Mashkovskii, G.N. Baeva, N.S. Telegina, Russ. J. Gen. Chem. 80 (2010) 618–629.
[60] P.W. Atkins, T.L. Overton, J.P. Rourke, M.T. Weller, F.A. Armstrong, Shriver and Atkins' Inorganic Chemistry, W.H. Freeman and Company, New York, 2010.
[61] M.J. Maccarrone, C.R. Lederhos, G. Torres, C. Betti, F. Coloma-Pascual, M.E. Quiroga, J.C. Yori, Appl. Catal. A: Gen. 441–442 (2012) 90–98.
[62] P.G.J. Koopman, Ruthenium Hydrogenation Catalysts, Delft University Press, Delft, 1980.
[63] R.M. Mironenko, O.B. Belskaya, V.A. Likholobov, Proc. 11th European Congress on Catalysis, EuropaCat-XI, Lyon, France, September 1st–6th, 2013.
[64] T.K. Shimizu, A. Mugarza, J.I. Cerdá, M. Heyde, Y. Qi, U.D. Schwarz, D.F. Ogletree, M. Salmeron, J. Phys. Chem. C 112 (2008) 7445–7454.
[65] M. Tatarkhanov, D.F. Ogletree, F. Rose, T. Mitsui, E. Fomin, S. Maier, M. Rose, J.I. Cerdá, M. Salmeron, J. Am. Chem. Soc. 131 (2009) 18425–18434.
[66] H. Rojas, G. Borda, D. Rosas, J.J. Martínez, P. Reyes, Dyna 75 (2008) 115–122.
[67] E.-J. Ras, S. Maisuls, P. Haesakkers, G.-J. Gruter, G. Rothenberg, Adv. Synth. Catal. 351 (2009) 3175–3185.
[68] P. Reyes, D. Salinas, C. Campos, M. Oportus, J. Murcia, H. Rojas, G. Borda, J.L.G. Fierro, Quím. Nova 33 (2010) 777–780.